J|A|C|S ARTICLES

Published on Web 12/02/2009

Naphthol Coupling Monitored by Infrared Spectroscopy in the Gas Phase

Jana Roithová*,†,‡ and Petr Milko‡

Department of Organic Chemistry, Charles University in Prague, Hlavova 8, 12843 Prague 2, Czech Republic, and Institute of Organic Chemistry and Biochemistry, Academy of Sciences of the Czech Republic, Flemingovo náměstí 2, 16610 Prague 6, Czech Republic

Received August 28, 2009; E-mail: roithova@natur.cuni.cz

Abstract: The reaction mechanism of copper(II)-mediated naphthol coupling in the presence of TMEDA (*N*,*N*,*N*′,*N*′-tetramethylethylenediamine) is studied using infrared multiphoton dissociation (IRMPD) spectroscopy and DFT calculations. It is shown that the coupling reaction proceeds in ad hoc formed binuclear clusters $[(\mathbf{1}\text{-H})_2Cu_2Cl(TMEDA)_2]^+$, where (**1**-H) is a deprotonated naphthol molecule (methyl ester of 3-hydroxy-2-naphthoic acid). The IRMPD spectra of the isolated cluster in the gas phase reveal that it contains two uncoupled naphtholate subunits and only the irradiation promotes the coupling reaction, which is thus observed as a genuine gas-phase reaction. The driving force for the C−C coupling is a keto−enol tautomerization of the initial coupling product, and the formation of the corresponding binol in the cluster is exothermic by 0.61 eV. In contrast, analogous C−O and O−O couplings are endothermic reactions.

Introduction

The mechanism of the oxidative C−C coupling of naphthols and related molecules mediated by transition metals is subject to an ongoing discussion. Most of the recently published highly enantioselective syntheses of BINOL and its derivatives are based on naphthol coupling catalyzed by chiral complexes containing two metal centers (vanadium, iron, or copper).[1−4] In consensus, the suggested mechanisms for these chemically bound binuclear catalysts are based on a formation of a complex between the catalysts and two molecules of naphthol, which thus couple in a highly chiral environment (Scheme 1). Interestingly, also formation of a self-dimerized chiral assembly of vanadium complexes on a SiO_2 surface was reported, which also promoted the enantioselective naphthol coupling.[5]

The mechanistic scenarios for the naphthol couplings mediated by transition metal salts or mononuclear transition metal complexes are more diverse. However, a generation of a free radical or a metal-bound radical from the naphthol reactant is usually involved as a central concept. The so-formed radical then reacts with another naphthol molecule from the reaction mixture.[3−9] In marked contrast to these scenarios, we have recently shown experimentally that, for copper-mediated naphthol coupling, various isolated complexes of copper(II) and naphtholate in the gas phase do not show any significant reactivity toward molecules sensitive to the carbon-centered radicals (e.g., CH_3I or $(CH_3S)_2$),[10] which therefore implies very low reactivity toward a nonactivated molecule of naphthol.[11] Instead, we have proposed a mechanism based on an ad hoc formation of binuclear clusters in the reaction mixture, where both molecules of naphthols are coordinated to metal centers and thus both molecules are activated for the coupling reaction. Such binuclear complexes can be identified by mass spectrometric analysis of reaction mixtures,[12−16] and the unimolecular reactivities of these binuclear complexes then suggest the formation of the coupled products.[11]

The mechanism has been suggested based on an electrospray-ionization mass spectrometric study[17,18] of copper(II)-mediated coupling of methyl ester of 3-hydroxy-2-naphthoic acid (**1**) in the presence of a nonchiral ligand TMEDA (*N*,*N*,*N*′,*N*′-tetramethylethylenediamine).[19] The use of the substituted naphthol **1** instead of 2-naphthol is implied by the kinetics of the coupling in solution: The coupling of 2-naphthol proceeds too fast, so

† Charles University in Prague.
‡ Academy of Sciences of the Czech Republic.

(1) (a) Luo, Z.; Liu, Q.; Gong, L.; Cui, X.; Mi, A.; Jiang, Y. *Angew. Chem., Int. Ed.* **2002**, *41*, 4532. (b) Guo, Q.-X.; Wu, Z.-J.; Luo, Z.-B.; Liu, Q.-Z.; Ye, J.-L.; Luo, S.-W.; Cun, L.-F.; Gong, L.-Z. *J. Am. Chem. Soc.* **2007**, *129*, 13927.
(2) (a) Somei, H.; Asano, Y.; Yoshida, T.; Takizawa, S.; Yamataka, H.; Sasai, H. *Tetrahedron Lett.* **2004**, *45*, 1841. (b) Takizawa, S.; Katayama, T.; Somei, H.; Asano, Y.; Yoshida, T.; Kameyama, C.; Rajesh, D.; Onitsuka, K.; Suzuki, T.; Mikami, M.; Yamataka, H.; Jayaprakash, D.; Sasai, H. *Tetrahedron* **2008**, *64*, 3361.
(3) Egami, H.; Katsuki, T. *J. Am. Chem. Soc.* **2009**, *131*, 6082.
(4) Gao, J.; Reibenspies, J. H.; Martell, A. E. *Angew. Chem., Int. Ed.* **2003**, *42*, 6008.
(5) Tada, M.; Taniike, T.; Kantam, L. M.; Iwasawa, Y. *Chem. Commun.* **2004**, 2542.
(6) Li, X.; Hewgley, J. B.; Mulrooney, C. A.; Yang, J.; Kozlowski, M. C. *J. Org. Chem.* **2003**, *68*, 5500.
(7) Hewgley, J. B.; Stahl, S. S.; Kozlowski, M. C. *J. Am. Chem. Soc.* **2008**, *130*, 12232.
(8) Smrčina, M.; Poláková, J.; Vyskočil, Š.; Kočovský, P. *J. Org. Chem.* **1993**, *58*, 4534.
(9) Temma, T.; Hatano, B.; Habaue, S. *Tetrahedron* **2006**, *62*, 8559, and references therein.
(10) Stirk, K. M.; Orlowski, J. C.; Leeck, D. T.; Kenttämaa, H. I. *J. Am. Chem. Soc.* **1992**, *114*, 8604.
(11) Roithová, J.; Schröder, D. *Chem.—Eur. J.* **2008**, *14*, 2180.
(12) Adlhart, C.; Chen, P. *Helv. Chim. Acta* **2000**, *83*, 2192.
(13) Chen, P. *Angew. Chem., Int. Ed.* **2003**, *42*, 2832.
(14) O'Hair, R. A. J. *Chem. Commun.* **2006**, 1469.
(15) Eberlin, M. N. *Eur. J. Mass Spectrom.* **2007**, *13*, 19.
(16) Santos, L. S. *Eur. J. Org. Chem.* **2008**, 235.

Scheme 1. General Mechanism for Naphthol Coupling Mediated by Binuclear Metal Complexes, Where Metal M Can Be Vanadium, Iron, Or Copper

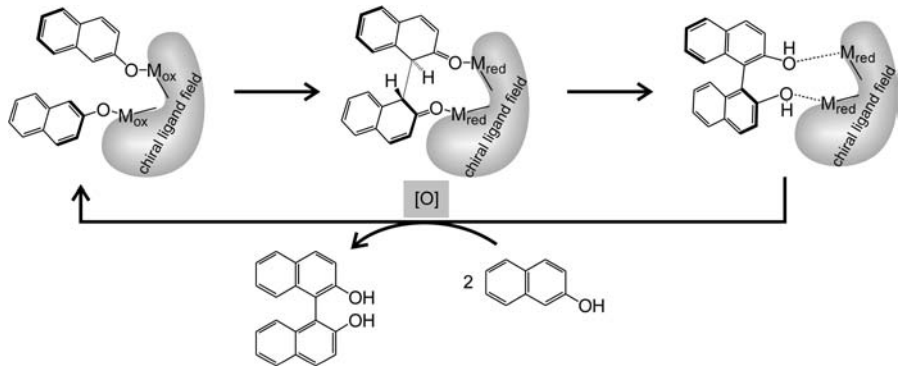

Scheme 2. Mechanism for Naphthol Coupling Mediated by a Binuclear Copper Complex, Where Metals Are Bound via a Counterion X (X = NO_3^-, Cl^-, or Br^-) and Each Metal Atom Bears a TMEDA Ligand and Deprotonated Naphthol **1**[11]

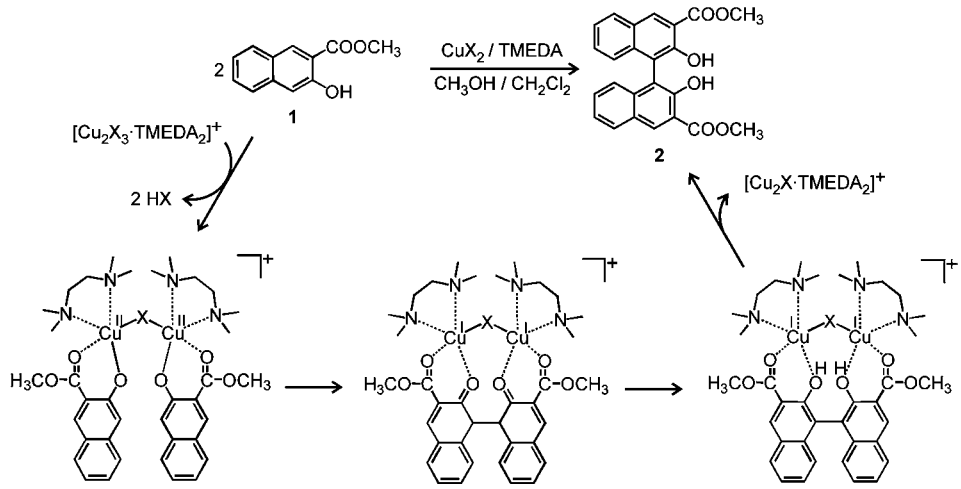

that only the binol product can be observed in the mass spectrometric experiment, whereas the electron-withdrawing ester function of **1** slows down the coupling and the reaction intermediates can be sampled from the reaction mixture.[12−16] The suggested mechanism for the naphthol coupling mediated by copper(II) in the presence of TMEDA is depicted in Scheme 2.[11]

Here, we will demonstrate that the oxidative coupling of two naphthol molecules in the binuclear copper clusters can be observed as a genuine gas-phase reaction as monitored by infrared multiphoton dissociation (IRMPD) spectroscopy.[20] A complementary study using density functional theory (DFT) reveals the identity of the intermediates and provides the underlying energetics for the suggested mechanism.

Experimental and Computational Details

The gas-phase infrared (IR) spectra of mass-selected ions were recorded using a Bruker Esquire 3000 ion trap mounted to a free-electron laser at CLIO (Centre Laser Infrarouge Orsay, France).[21] The laser was operated in the 40−45 MeV electron-energy range and it provided light in a 1000−1800 cm^{-1} range. The ions of interest were generated from a CH_2Cl_2/CH_3OH solution of [Cu(OH)Cl(TMEDA)] and the methyl ester of 3-hydroxy-2-naphthoic acid (or its binol) by electrospray ionization, were mass-selected, and were stored in the ion trap. The fragmentation was induced by one to four laser pulses admitted to the ion trap, and the dependence of the fragmentation intensities on the wavelength of the IR light gives the infrared multiphoton dissociation (IRMPD) spectra. The power of the free-electron laser slightly decreases with increasing wavenumbers (see the Supporting Information); the reported IRMPD spectra are averages of two or three raw spectra and are not corrected for the power of the free-electron laser.

In contrast to most mass spectrometric methods, IRMPD provides direct experimental information about structures of ions in the gas phase. The technique consists in the fragmentation of mass-selected ions in a storage cell by a tunable infrared laser. The ions can be fragmented only if they can absorb photons of a given energy, which means that the photons have to correspond to an arbitrary transition

(17) For selected mass-spectrometric mechanistic studies see: (a) Santos, L. S.; Pavam, C. H.; Almeida, W. P.; Coelho, F.; Eberlin, M. N. *Angew. Chem., Int. Ed.* **2004**, *43*, 4330. (b) Waters, T.; Khairallah, G. N.; Wimala, S. A. S. Y.; Ang, Y. C.; O'Hair, R. A. J.; Wedd, A. G. *Chem. Commun.* **2006**, 4503. (c) Chiavarino, B.; Cipollini, R.; Crestoni, M. E.; Fornarini, S.; Lanucara, F.; Lapi, A. *J. Am. Chem. Soc.* **2008**, *130*, 3208. (d) Torker, S.; Merki, D.; Chen, P. *J. Am. Chem. Soc.* **2008**, *130*, 4808. (e) Schrader, W.; Handayani, P. P.; Zhou, J.; List, B. *Angew. Chem., Int. Ed.* **2009**, *48*, 1463.

(18) Roithová, J.; Schröder, D. *Coord. Chem. Rev.* **2009**, *253*, 666.

(19) (a) Noji, M.; Nakajima, M.; Koga, K. *Tetrahedron Lett.* **1994**, *35*, 7983. (b) Nakajima, M.; Miyoshi, I.; Kanayama, K.; Hashimoto, S.; Masahiro, N.; Koga, K. *J. Org. Chem.* **1999**, *64*, 2264.

(20) (a) MacAleese, L.; Maitre, P. *Mass Spectrom. Rev.* **2007**, *26*, 583, and references therein. (b) Polfer, N. C.; Oomens, J. *Mass Spectrom. Rev.* **2009**, *28*, 468.

(21) Mac Aleese, L.; Simon, A.; McMahon, T. B.; Ortega, J. M.; Scuderi, D.; Lemaire, J.; Maitre, P. *Int. J. Mass Spectrom.* **2006**, *249*, 14–20.

$v = 0 \rightarrow v = 1$ in the studied ion. The dependence of the fragmentation yield on the wavelength of the laser provides a link to the infrared spectrum of the isolated ion. For structure elucidation, usually a comparison of the IRMPD spectrum with a theoretical IR spectrum is made and a positive assignment requires a match of all measured IRMPD bands with the calculated spectrum. The obtained intensities of the IRMPD bands do not however exactly correspond to the theoretical IR intensities, and some bands can even disappear in the experimental spectrum.[22,23] The fragmentation is obviously associated with a sufficient amount of energy absorbed by the parent ion, but also with the efficient intramolecular vibrational redistribution, which allows a repetitive photon absorption by the $v = 0 \rightarrow v = 1$ transition. Dissociation of an ion can be usually achieved only after absorption of several IR photons, which challenges the linear relationship between the conventional IR intensities and intensities of bands measured in the IRMPD spectrum. All details of mechanisms influencing the appearance of the IRMPD spectra remain still to be uncovered.[20]

The computational DFT study was performed using the B3LYP[24−27] functional as implemented in the Gaussian 03 package.[28] Basis sets 6-31G*, TZVP, and a combination of 6-311+G* for copper and 6-31G* for all other atoms (denoted as 6-311+G*:6-31G* in the following) were tested.[29] We found that using the combination of the 6-311+G*:6-31G* basis sets leads to a good agreement in relative energetics and geometries with the results obtained for the structures optimized at the best B3LYP/TZVP level tested (Table S1 in the Supporting Information). On the other hand, the energetics obtained using the smallest basis set 6-31G* is significantly different from those obtained with larger basis sets. Further, we found that the 6-31G* basis set completely fails for the description of the closed-shell singlet binuclear clusters. As far as the calculated IR spectra are concerned, all methods provide very similar results, if the geometries are similar (thus with exception of closed-shell binuclear clusters). As a compromise, we have thus chosen optimization at the B3LYP/6-311+G*:6-31G* level followed by a single-point calculation at the B3LYP/TZVP level. Zero-point energies and IR spectra were calculated at the B3LYP/6-311+G*:6-31G* level. The calculated frequencies were scaled by a factor of 0.9613 for copper(I) species and 0.95 for copper(II) species,[30,31] if not stated otherwise (see figure captions). The biradical dicopper complexes were optimized at the triplet states, and the energies of the corresponding biradical singlet states were obtained by single-point calculations at the UB3LYP/TZVP level and applying a broken symmetry correction:[32] $J_{12} = 2(E_{HS} - E_{BS})/(\langle S^2\rangle_{HS} - \langle S^2\rangle_{BS})$,[33] where HS corresponds to the triplet state and BS corresponds to the UB3LYP calculated energy for the open-shell low-spin state. The J_{12} values found for various conformers of the complex $\mathbf{3}^+$ range from −0.04 to 0.13 eV. These values are at the border of accuracy expected for the method applied; therefore we discuss only energies of the triplet states in the following, whereas the singlet state energies are listed together with more details about the choice of the method in the Supporting Information.

Results and Discussion

In a previous experimental study about the mechanism of the copper catalyzed naphthol coupling, the mono- and binuclear species evolving from the reaction solution of naphthol **1** (methyl ester of 3-hydroxy-2-naphthoic acid) and Cu(OH)Cl·TMEDA were probed with respect to their connection to the coupling process. As mentioned in the Introduction, the binuclear cluster $[(\mathbf{1}\text{-H})_2Cu_2Cl(TMEDA)_2]^+$ has been suggested to carry the coupling reaction. Collision induced dissociation of the mass-selected cluster $[(\mathbf{1}\text{-H})_2Cu_2Cl(TMEDA)_2]^+$ in the tandem (triple quadrupole) mass spectrometer[34] revealed three major dissociation channels: cluster cleavage to $[(\mathbf{1}\text{-H})Cu(TMEDA)]^+ + [(\mathbf{1}\text{-H})CuCl(TMEDA)]$, elimination of TMEDA, and elimination of $(\mathbf{1}\text{-H})_2$. Comparison with the reactivity of the monomeric complex $[(\mathbf{1}\text{-H})Cu(TMEDA)]^+$ and the corresponding binol complexes led to the unambiguous conclusion that the elimination of $(\mathbf{1}\text{-H})_2$ from $[(\mathbf{1}\text{-H})_2Cu_2Cl(TMEDA)_2]^+$ corresponds to the formation of a coupled molecule, rather than consecutive losses of two naphthoxy units.[11] Although it was shown that the binol molecule (**2**) was not formed in the solution, the coupling promoted under the electrospray conditions was difficult to exclude. In other words, the mass-selected ions did not need to correspond only to $[(\mathbf{1}\text{-H})_2Cu_2Cl(TMEDA)_2]^+$, but also isobaric complex $[(\mathbf{2})Cu_2Cl(TMEDA)_2]^+$ could have been present. In order to resolve this dilema, the structures of ions in the gas phase are investigated by infrared multiphoton dissociation (IRMPD) spectroscopy (see Experimental and Computational Details). We will first address the monomeric complex $[(\mathbf{1}\text{-H})Cu(TMEDA)]^+$ and the complexes of binol **2** (4,4′-bi-3-hydroxy-2-methylnaphthoate), $[(\mathbf{2}\text{-H})Cu(TMEDA)]^+$ and $[(\mathbf{2}\text{-2H})Cu_2Cl(TMEDA)_2]^+$, in order to understand some general features in the IRMPD spectra of these compounds. With this knowledge we will approach the complex of interest, $[(\mathbf{1}\text{-H})_2Cu_2Cl(TMEDA)_2]^+$, and elucidate the mechanism of the coupling reaction.

The experimental spectrum of $[(\mathbf{1}\text{-H})Cu(TMEDA)]^+$ agrees well with the theoretical spectrum obtained for the complex, where both, naphtholate and TMEDA are bound as bidentate ligands to the copper ion (Figure 1). Figure 1a and 1b show the effects of the basis sets TZVP and 6-311+G*:6-31G*, respectively, on the computed spectra. Both predictions are in very good agreement with the experimental spectrum in the 1200−1500 cm^{-1} range (mostly stretching modes of the single bonds). The IRMPD band at about 1570 cm^{-1} corresponding most probably to the carbonyl vibration is predicted at slightly lower wavelengths using both basis sets. For the following larger complexes, only the basis set 6-311+G*:6-31G* is used.

We have shown previously that, for the phenolate/Cu(II) system ($[PhOCu]^+$), the wavelength of the stretching vibration of the C−O bond is a sensitive marker for the transfer of the radical site from copper(II) to the aromatic ring: The stretching vibration of the C−O bond around 1500 cm^{-1} corresponds to the localization of the radical site at the aromatic ring, whereas its red shift to about 1300 cm^{-1} indicates localization of the

(22) Schröder, D.; Schwarz, H.; Milko, P.; Roithová, J. *J. Phys. Chem. A* **2006**, *110*, 8346.
(23) Simon, A.; Joblin, Ch.; Polfer, N.; Oomens, J. *J. Phys. Chem. A* **2008**, *112*, 8551.
(24) Vosko, S. H.; Wilk, L.; Nusair, M. *Can. J. Phys.* **1980**, *58*, 1200.
(25) Lee, C.; Yang, W.; Parr, R. G. *Phys. Rev. B* **1988**, *37*, 785.
(26) Becke, A. D. *Phys. Rev. A* **1988**, *38*, 3098.
(27) Becke, A. D. *J. Chem. Phys.* **1993**, *98*, 5648.
(28) Frisch, M. J.; et al. *Gaussian 03*, Revision C.02; Gaussian, Inc.: Wallingford, CT, 2004.
(29) For other B3LYP calculations on copper complexes see: (a) Alcamí, M.; Alberto, L.; Mó, O.; Yánez, M.; Tortajada, J.; Amekraz, B. *Chem.−Eur. J.* **2004**, *10*, 2927. (b) DeChancie, J.; Acevedo, O.; Evanseck, J. D. *J. Am. Chem. Soc.* **2004**, *126*, 6043. (c) Poater, A.; Ribas, X.; Llobet, A.; Cavallo, L.; Sola, M. *J. Am. Chem. Soc.* **2008**, *130*, 17710.
(30) Merrick, J. P.; Moran, D.; Radom, L. *J. Phys. Chem. A* **2007**, *111*, 11683.
(31) A smaller scaling factor for copper(II) species than for copper(I) species were observed before. See ref 35.
(32) (a) Noodleman, L.; Norman, J. G., Jr. *J. Chem. Phys.* **1979**, *70*, 4903. (b) Noodleman, L. *J. Chem. Phys.* **1981**, *74*, 5737.
(33) Nishino, M.; Yamanaka, S.; Yoshioka, Y.; Yamaguchi, K. *J. Phys. Chem. A* **1997**, *101*, 705.
(34) Roithová, J.; Schröder, D.; Míšek, J.; Stará, I. G.; Starý, I. *J. Mass Spectrom.* **2007**, *42*, 1233.

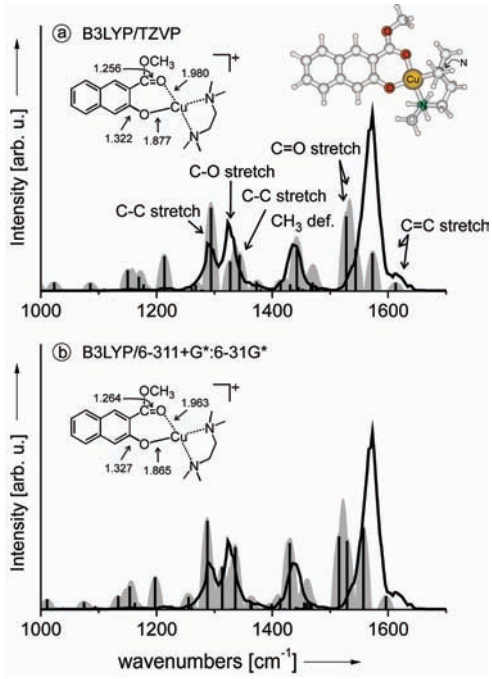

Figure 1. IRMPD spectra (black lines) of the $[(\mathbf{1}\text{-H})Cu(TMEDA)]^+$ complex compared with theoretical IR spectra (black bars) of the most stable structure of the corresponding complex calculated (a) at the B3LYP/TZVP level (scaling factor 0.97, the maximum theoretical intensity $I_{max} = 362$ km/mol) and (b) at the B3LYP/6-311+G*:6-31G* level (scaling factor 0.95, $I_{max} = 318$ km/mol). The gray areas show the theoretical spectra folded with Gaussian peak shapes with fwhm (full width at half-maximum) of 20 cm^{-1}. The "ball and stick" model shows a view on the optimized geometry; copper is given in yellow, oxygen in red, nitrogen in green, and carbon and hydrogen atoms in gray. The lengths of the C−O and O−Cu bonds are given in angstroms.

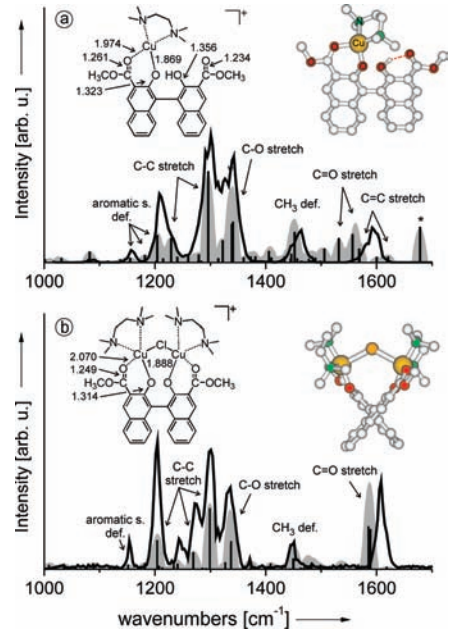

Figure 2. IRMPD spectra (black lines) of (a) $[(\mathbf{2}\text{-H})Cu(TMEDA)]^+$ and (b) $[(\mathbf{2}\text{-2H})Cu_2Cl(TMEDA)_2]^+$ and their comparison with theoretical IR spectra (black bars, scaling factors 0.966, $I_{max} = 652$ km/mol and $I_{max} = 658$ km/mol, respectively) of the most stable structures of the corresponding complexes. The gray areas show the theoretical spectra folded with Gaussian peak shapes with fwhm (full width at half-maximum) 20 cm^{-1}. The "ball and stick" models show a view on the optimized geometries of the corresponding complexes; copper is given in yellow, chlorine in orange, oxygen in red, nitrogen in green, and carbon atoms in gray; the hydrogen atoms have been removed. The lengths of the C−O and O−Cu bonds are given in angstroms.

nonpaired electron at the copper ion.[35,36] The former situation corresponds to the reduction of Cu(II) to Cu(I), and it is only realized if no ligands or a single additional ligand is attached to the $[PhOCu]^+$ core, because Cu(I) strongly prefers a linear coordination.[37] On the other hand, two or more additional ligands stabilize the oxidation state Cu(II) and phenolate remains in its reduced form.

Two bidentate ligands bound to the copper ion in the complex $[(\mathbf{1}\text{-H})Cu(TMEDA)]^+$ are arranged in a distorted tetrahedral geometry. Thus, already the geometry suggests that copper keeps the oxidation state (II). Analysis of the theoretical spectrum reveals that the C−O stretching vibration of the naphtholic group is located at 1320 cm^{-1}, which demonstrates the closed-shell character of the naphtholate group. Consistent with this conclusion, the spin density at the aromatic moiety ($C_{10}H_6$) amounts to 0.04 e (Mulliken analysis at the B3LYP/TZVP level). This finding is in agreement with the previous experimental results which showed that the complex of naphtholate and copper(II) is not reactive toward dimethyl disulfide and other sensitive reagents toward the carbon-centered radicals.

In order to probe the putative product of the C−C coupling step, also the binol **2** is investigated. The most stable structure found for the complex of binolate $(\mathbf{2}\text{-H})^-$, copper, and TMEDA is analogous to $[(\mathbf{1}\text{-H})Cu(TMEDA)]^+$. The copper ion is in distorted tetrahedral geometry coordinated to one of the naphthol subunits and to TMEDA (Figure 2a). The experimental IRMPD data are well reproduced by the corresponding calculated spectrum up to 1500 cm^{-1}. However, the C═O and C═C vibrations are again predicted at slightly lower wavenumbers than observed in the experiment. Interestingly, the carbonyl vibration of the noncoordinated ester function (1678 cm^{-1}, denoted by an asterisk in Figure 2a) does not appear in the experimental spectrum at all. It might be simply explained as an experimental artifact due to the decreasing intensity of the free-electron laser with increasing wavenumbers (Figure S1 in the Supporting Information). However, this phenomenon can also point toward a more fundamental difference between the coordinated and noncoordinated carbonyl groups. Specifically, different capabilities of the two carbonyl groups in the internal vibrational redistribution (IVR) process can be suggested and this effect forms a challenge for forthcoming studies. We note in passing that structures with copper being coordinated to both ester functions are not possible because of the spatial distance of the carbonyl groups.

Next to the mononuclear copper complex of binol **2**, also binuclear complexes are formed. The most abundant binuclear complex contains doubly deprotonated binol bound to two copper ions. Each copper ion bears a TMEDA ligand, and the complex contains also a chlorine atom as a counterion. In the most stable structure found for this complex (see a view at Figure 2b), chloride forms a bridge between two copper ions. A structure in which the bridge is broken and the chlorine anion is bound only to one of the copper cations lies 0.41 eV higher

(35) Milko, P.; Roithová, J.; Tsierkezos, N.; Schröder, D. *J. Am. Chem. Soc.* **2008**, *130*, 7186.
(36) Milko, P.; Roithová, J.; Schröder, D.; Lemaire, J.; Schwarz, H.; Holthausen, M. C. *Chem.—Eur. J.* **2008**, *14*, 4318.
(37) (a) Chaboy, J.; Munoz-Paez, A.; Merkling, P. J.; Marcos, E. S. *J. Chem. Phys.* **2006**, *124*, 064509. (b) Inoue, K.; Ohashi, K.; Iino, T.; Judai, K.; Nishi, N.; Sekiya, H. *Phys. Chem. Chem. Phys.* **2007**, *9*, 4793.

Chart 1

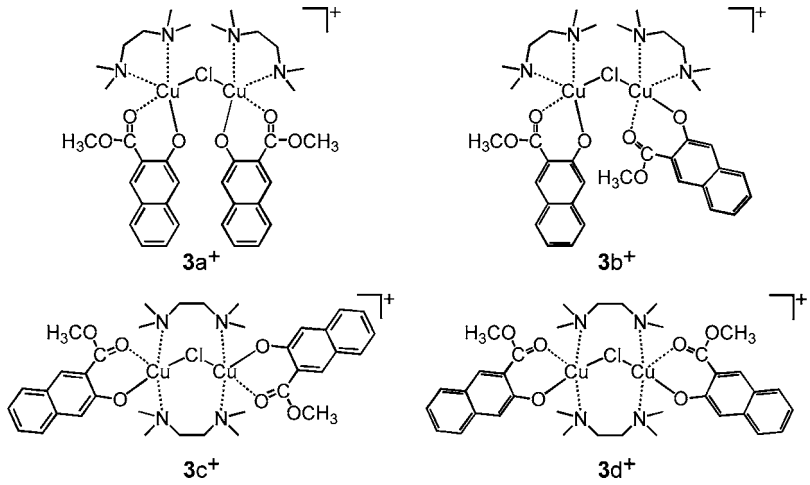

in energy. The calculated spectrum for the most stable structure agrees well with the experimental IRMPD spectrum; only the band corresponding to the stretching modes of the double bonds is again predicted at lower wavenumbers. For comparison, the IR spectrum of the more energetic isomer contains two separated bands at 1558 and 1612 cm^{-1} for the C═O bands of the two nonequivalent carbonyl groups, which is not observed in the experimental spectrum.

The comparison of all spectra in Figures 1 and 2 reveals two important findings. First, the binol skeleton shows more intense bands of C−C and C−O single bonds in the range of about 1180−1350 cm^{-1} compared to the bands of double bonds in the range of about 1550−1650 cm^{-1}, whereas the opposite is found for the naphthol complex. In particular, the intense band at about 1200 cm^{-1} seems to be a spectral sign of the larger system. Second, the coordination of the copper ion to the carbonyl group of the ester function has a decisive impact on the intensity of the C═O band with respect to other bands in the spectrum. Thus, from the relative intensities of the C═O bands and other bands in the IRMPD spectrum, it can be estimated whether both ester functions or rather only one of them is coordinated to the metal center.

Finally, a cluster with two units of the naphtholate/copper/TMEDA complex $[(\mathbf{1}\text{-H})Cu(TMEDA)]^+$ bound via chloride is investigated (Chart 1). The calculations show that the coordination of naphtholate and TMEDA to the copper ion in the two subunits has almost a square planar geometry. Two orientations of the $[(\mathbf{1}\text{-H})Cu(TMEDA)]^+$ subunits can be considered ($\mathbf{3}a^+$ and $\mathbf{3}b^+$ in Chart 1), and several minima for each orientation can be found if we consider a rotation of one $[(\mathbf{1}\text{-H})Cu(TMEDA)]^+$ subunit around the axis going through both copper ions. All located minima lie very close in energy (with the energy differences smaller than 0.1 eV), and therefore it can be expected that the investigated cluster ion is rather floppy in the gas phase. The most stable structure corresponds to the isomer $\mathbf{3}a^+$, and $\mathbf{3}b^+$ lies 0.04 eV higher in energy. For the sake of completeness, we have investigated also structures in which TMEDA operates as a bridging ligand ($\mathbf{3}c^+$ and $\mathbf{3}d^+$ in Chart 1), but these isomers lie more than 1.3 eV higher in energy than the isomers with chelating TMEDA ligands. The calculated IR spectra of all optimized structures of $\mathbf{3}^+$ are very similar in that the positions of individual bands do not differ more than a few wavenumbers.

The experimental IRMPD spectrum obtained for the cluster $[(\mathbf{1}\text{-H})_2Cu_2Cl(TMEDA)_2]^+$ shows features similar to those of spectra reported above. In comparison with the theoretical spectra of $\mathbf{3}a^+$ and $\mathbf{3}b^+$, the observed bands can be assigned (Figure 3). The broad band centered at about 1600 cm^{-1} is attributed to the C═C and C═O vibrations. Similarly to other calculated spectra discussed above, the vibrational modes of the double bonds are predicted at slightly lower wavenumbers than observed experimentally. The band at about 1430 cm^{-1} corresponds to the deformation vibration of the methyl group, the overlapping bands from about 1220 to 1390 cm^{-1} represent

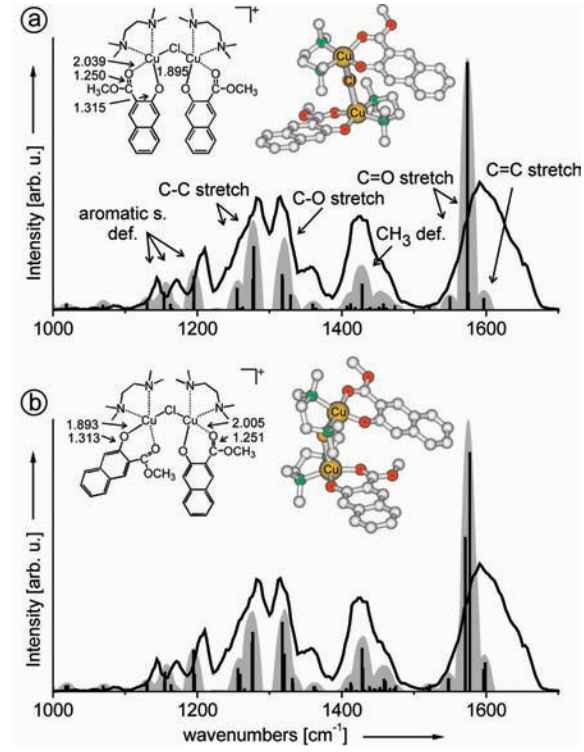

Figure 3. IRMPD spectrum (black solid lines) of the $[(\mathbf{1}\text{-H})_2Cu_2Cl(TMEDA)_2]^+$ complex. Comparison of the experimental spectra with the theoretical IR spectra (black bars, scaling factor 0.95) of the most stable structures of (a) $\mathbf{3}a^+$ and (b) $\mathbf{3}b^+$. The gray areas show the theoretical spectra folded with Gaussian peak shapes with fwhm of 20 cm^{-1}. The "ball and stick" models show a view on the optimized geometries of the corresponding complexes; copper is given in yellow, chlorine in orange, oxygen in red, nitrogen in green, and carbon atoms in gray; the hydrogen atoms have been removed. The lengths of the C−O and O−Cu bonds are given in angstroms. The maximum theoretical IR intensities are I_{max} = 1651 km/mol and I_{max} = 1124 km/mol, respectively.

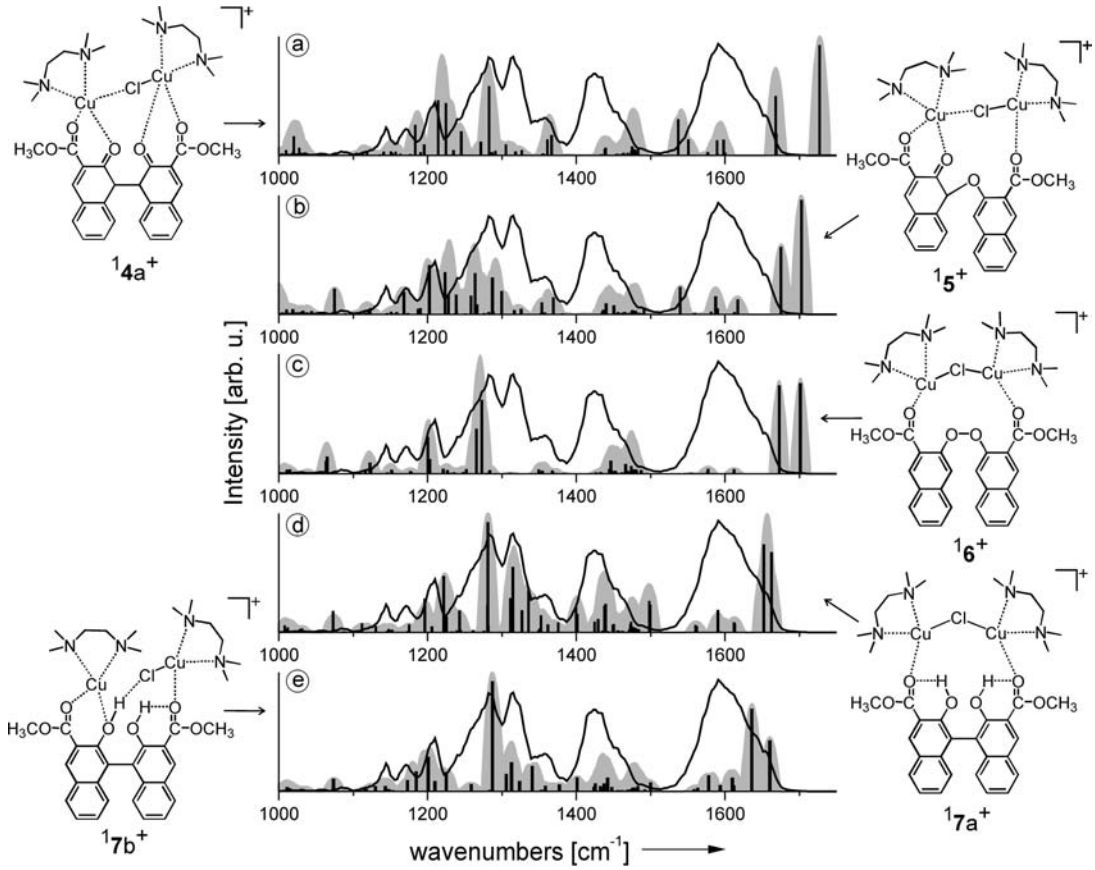

Figure 4. Comparison of IRMPD spectra of the $[(\mathbf{1}\text{-H})_2Cu_2Cl(TMEDA)_2]^+$ (black solid lines) with calculated spectra (scaling factors 0.9613, I_{max} given in brackets) of the primary coupled products (a) $^1\mathbf{4}^+$ (I_{max} = 589 km/mol), (b) $^1\mathbf{5}^+$ (I_{max} = 625 km/mol), and (c) $^1\mathbf{6}^+$ (I_{max} = 447 km/mol), and the enol forms of the C−C coupled product products (d) $^1\mathbf{7}a^+$ (I_{max} = 483 km/mol) and (e) $\mathbf{7}b^+$ (I_{max} = 781 km/mol).

C−C and C−O vibrations, and finally the bands at 1140, 1170, and 1200 cm^{-1} correspond to the deformation vibrations of the aromatic systems. The experimental and theoretical spectra are in very good agreement, although the C═O stretching mode is again predicted at slightly lower wavenumbers and the same is true for three bands corresponding to the deformation vibrations of the aromatic system.

Figure 3b demonstrates that the calculated IR spectra are not sensitive to the actual conformation of the $[(\mathbf{1}\text{-H})_2Cu_2Cl(TMEDA)_2]^+$ complex. The IR spectrum of the most stable structure found for isomer $\mathbf{3}b^+$ is almost identical with that of $\mathbf{3}a^+$. Even the spectrum of a structurally very different, high-energy isomer with the TMEDA ligands acting as bridging ligands has very similar appearance (see Supporting Information). The small differences between the spectra in conjunction with the sampling of a mixture of low-energy conformations can account for a seemingly lower resolution of this IRMPD spectrum compared to the spectra mentioned above.

The IR spectra of possible complexes with the same mass, but containing the coupled product, are shown in Figure 4. None of the spectra is in agreement with experiment. On one hand, the possible primary coupled products corresponding to the keto form of the C−C coupled product $\mathbf{4}^+$, the keto form of the C−O coupled product $\mathbf{5}^+$, and the O−O coupled product $\mathbf{6}^+$ have completely different band structures in the range of stretching vibrations of single bonds (ca. 1200−1400 cm^{-1}) and in particular the band at 1315 cm^{-1}, which corresponds to the C−O stretching mode, is not reproduced at all. None of the theoretical spectra of all possible coupled products, including more stable enol foms of the C−C coupled product $^1\mathbf{7}a^+$ and $^1\mathbf{7}b^+$, reproduces the experimental band at 1570 cm^{-1}, which is consistent with the interpretation of this band as a carbonyl stretching mode of the ester function coordinated to copper(II). As all coupled products contain copper(I) ions, the appearance of the IR spectra in this range is completely different. Note also that neither increasing nor decreasing of the scaling factor applied to the theoretical vibrations leads to agreement between any of the theoretical spectra and the IRMPD spectrum.

In summary, we conclude that the ion isolated in the gas phase corresponds to the complex $[(\mathbf{1}\text{-H})_2Cu_2Cl(TMEDA)_2]^+$ with two isolated naptholate units and the observed elimination of the coupled product $(\mathbf{1}\text{-H})_2$ is induced either by irradiation (here) or collision (in previous work) and the coupling is therefore observed as a genuine gas-phase reaction.

Based on our calculations and structure verifications by IRMPD spectroscopy, we therefore suggest the following reaction mechanism for the oxidative coupling of two naphthol molecules (Figure 5). The reactive complex $\mathbf{3}^+$, i.e., $[(\mathbf{1}\text{-H})_2Cu_2Cl(TMEDA)_2]^+$, is formed ad hoc in solution by binding of monomeric units $[(\mathbf{1}\text{-H})CuCl(TMEDA)]$ and $[(\mathbf{1}\text{-H})Cu(TMEDA)]^+$, or by an exchange of chlorine atoms by the naphthoxy units in $[Cu_2Cl_3(TMEDA)_2]^+$ or $[(\mathbf{1}\text{-H})Cu_2Cl_2(TMEDA)_2]^+$. We note in passing that all these species including the investigated complex $[(\mathbf{1}\text{-H})_2Cu_2Cl(TMEDA)_2]^+$ are sampled directly from the reactive solution. The C−C coupling between two naphthoxy units within the reactive complex $[(\mathbf{1}\text{-H})_2Cu_2Cl(TMEDA)_2]^+$ ($^3\mathbf{3}^+$) is endothermic by 0.96 eV and leads to the keto form of the binol product coordinated to the $[Cu_2Cl(TMEDA)]^+$ cluster ($^1\mathbf{4}a^+$). This isomer can relax by opening one Cu−Cl bond to a more stable form $^1\mathbf{4}b^+$, which

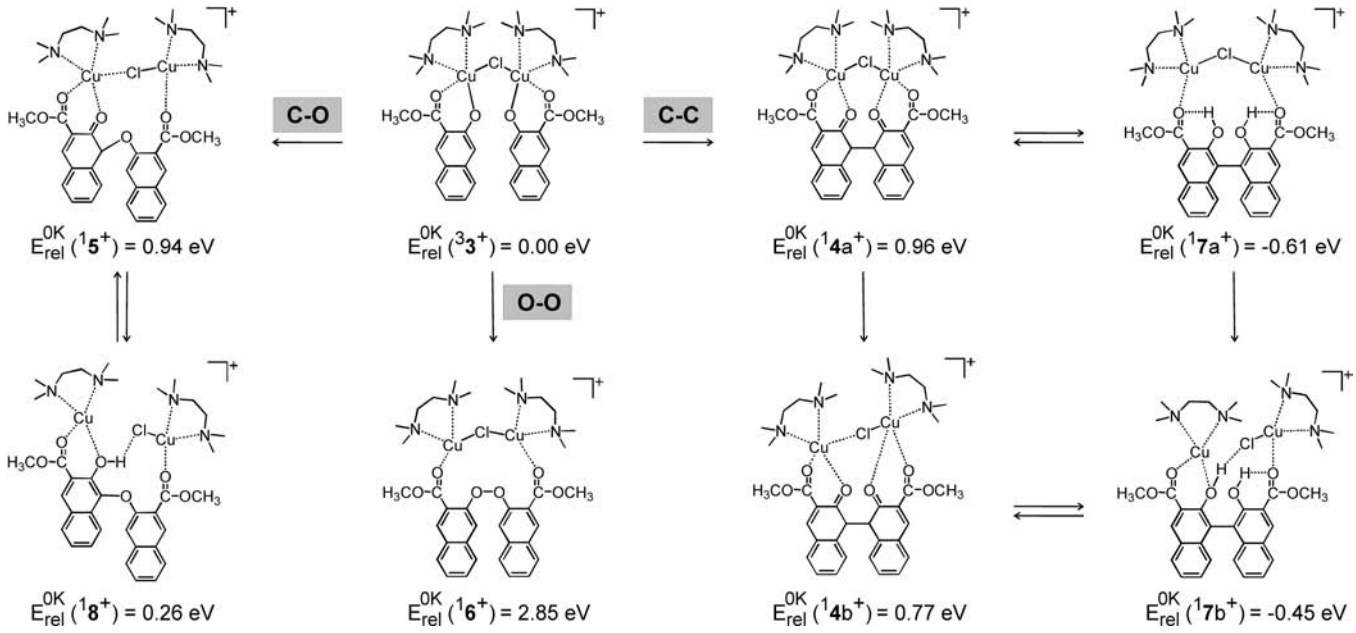

Figure 5. B3LYP/TZVP//B3LYP/6-311+G*:6-31G* calculations of the oxidative coupling of two naphthol molecules **1** catalyzed by copper(II) and TMEDA.

contains one tightly coordinated copper ion and a [CuCl-(TMEDA)] unit coordinated loosely. Note that the starting complex is a biradical with two radical sites located at the copper atoms, whereas the product is a closed-shell molecule. The equilibrium between the coupled and uncoupled products is driven toward the formation of binol by the subsequent keto−enol tautomerization, which is exothermic by 1.57 eV, and the overall coupling reaction is thus exothermic by 0.61 eV.

In comparison, the formation of the concurrent primary C−O coupling product $^1\mathbf{5}^+$ requires similar energy ($E_{rel}{}^{0\,K}(^1\mathbf{5}^+) = 0.94$ eV), but the subsequent keto−enol tautomerization leads still to an endothermic product $^1\mathbf{8}^+$ with an overall energy demand of 0.26 eV. Finally, the O−O coupling is endothermic by 2.85 eV and therefore cannot compete with the major C−C coupling route.

The detailed analysis of the structures of the C−C coupled products gives further rationale for the observed fragmentation channels of mass-selected $[(\mathbf{1}\text{-H})_2Cu_2Cl(TMEDA)_2]^+$. Figure 6 shows a mass spectrum obtained by the integration of all peaks in the IRMPD spectrum of $[(\mathbf{1}\text{-H})_2Cu_2Cl(TMEDA)_2]^+$ for the individual observed fragmentations. We note in passing that IRMPD spectra derived independently from the individual fragmentation channels are the same within experimental error, which is yet another hint that the parent ions correspond to $\mathbf{3}^+$ exclusively, rather than a mixture of noninterconverting isomers. Interestingly, the relative abundances of fragmentation channels dramatically differ from those observed earlier in the collision induced dissociation spectrum of $[(\mathbf{1}\text{-H})_2Cu_2Cl(TMEDA)_2]^+$.[11] Fragmentation induced by IR irradiation leads much less to the cluster cleavage (formation of $[(\mathbf{1}\text{-H})Cu(TMEDA)]^+ + [(\mathbf{1}\text{-H})CuCl(TMEDA)]$), and instead the channels corresponding to the coupling reaction prevail (see below). This can be easily understood, because the IR irradiation leads to a slow increase of internal energy of the parent ions,[38] which provides time for the necessary rearrangements associated with the coupling reaction, and hence this thermodynamically favored process can prevail. In contrast, a collision induced dissociation (CID) experiment leads to kinetically favored products.

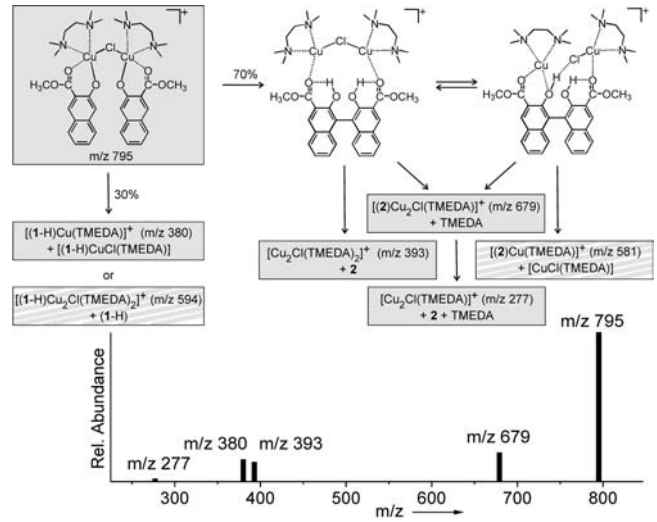

Figure 6. Mass spectrum obtained by the integration of peaks in the IRMPD spectrum of $[(\mathbf{1}\text{-H})_2Cu_2Cl(TMEDA)_2]^+$ independently for all fragmentation channels observed and the interpretation of the fragmentation channels. The channels in the hatched frames were observed only in the CID experiment.[11]

For illustration of these various aspects, let us consider a deconvolution of the mass spectrum to the processes associated either with the degradation of the cluster or with the coupling reaction. The cluster cleavage (evidenced by *m*/*z* 380) and the elimination of one naphthoxy unit (*m*/*z* 594; minor channel observed only under the CID conditions) clearly result from the direct fragmentation of the original uncoupled product $\mathbf{3}^+$ (Figure 6). All other fragmentation channels lead via the primary coupling $\mathbf{3}^+ \rightarrow \mathbf{4}^+$, where these channels include the elimination of TMEDA, [CuCl(TMEDA)] (only in the CID experiment), loss of the coupled product **2**, and the combined elimination of TMEDA and **2** (peaks at *m*/*z* 679, 581, 393, and 277,

(38) McLuckey, S. A.; Goeringer, D. E. *J. Mass Spectrom.* **1997**, *32*, 461.

respectively). The C−C coupled product can be formed in two stable isomers: the first one, ^{1}**7**a^{+}, with a conserved Cu−Cl−Cu bridge will lead directly to the elimination of the binol product. In the second isomer, ^{1}**7**b^{+}, the copper units are separated and therefore this isomer can lose neutral [CuCl(TMEDA)]. Both isomers will easily lose the TMEDA ligand, because as noted above the copper(I) ion is preferentially linearly coordinated and the binding energies for additional ligands are small (on the contrary, the original parent ions with two uncoupled naphthoxy units should rather lose the naphthoxy ligand than TMEDA).[11] Based on this deconvolution of the mass spectrum, the branching ratio between the cluster degradation (D) and the coupling reaction (R) can be estimated. Thus, under the IRMPD conditions the ratio D:R amounts to 30%:70%, whereas the ratio in the previous CID experiment can be estimated as 60%:40%, respectively.

Conclusions

Using IRMPD spectroscopy and DFT calculations, we have shown that the oxidative coupling of two naphthol molecules mediated by copper(II) proceeds in binuclear clusters, where both naphthoxy units to be coupled are activated by binding to their own copper(II) center. The ad hoc formed complexes [(**1**-H)$_2$Cu$_2$Cl(TMEDA)$_2$]$^{+}$ can be sampled by ESI mass spectrometry. The IRMPD spectrum of the complex clearly reveals that it contains two isolated naphthoxy units and copper(II) centers. The coupling observed in the unimolecular fragmentation is therefore induced by a collision or an absorption of IR photons and therefore constitutes a genuine gas-phase reaction. The theoretical investigation of the system shows that the formation of the primary C−C coupled product in the keto form is endothermic by 0.96 eV and the following keto−enol tautomerization is exothermic by 1.57 eV. The overall C−C coupling is therefore exothermic by 0.61 eV and the keto−enol tautomerization provides the driving force for the reaction. On the contrary, both the C−O coupling and the O−O coupling are endothermic reactions and therefore are energetically disfavored.

Knowledge of reaction mechanisms is the most important step toward the rational design of suitable catalysts and conditions. It has already been shown experimentally that chiral chemically bound binuclear metal clusters are superior to mononuclear metal complexes or metal salts as far as enantioselectivity and yields are concerned. However, the combination of metal salts and chiral ligands will most probably stay the economically preferred variant. The enantioselectivity and yield can be thus improved by a selection of better bridging counterions or a solvent supporting the clustering. We believe that the binuclear mechanism of naphthol coupling is not an exception, but similar reactivity can be observed also for other oxidation reactions, where copper(II) is involved as a mediator.

Acknowledgment. Dedicated to Prof. Miloslav Černý on the occation of his 80th birthday. The authors thank the Grant Agency of the Academy of Sciences of the Czech Republic (KJB400550704), the Ministry of Education of the Czech Republic (MSM0021620857, RP MSMT 14/63), and the European Commission for travel grants to the European multiuser facility CLIO. The authors thank Joël Lemaire for kind assistance during the measurements at CLIO.

Supporting Information Available: More details on the theoretical approach chosen, total energies, optimized geometries, dependence of free-electron laser intensity on the wavelength during measurements, and complete ref 28. This material is available free of charge via the Internet at http://pubs.acs.org/.

JA907291D